

50-day Oscillation of Length-of-day Change

Lihua Ma · Yanben Han · Dechun Liao

Received: 7 June 2007 / Accepted: 5 February 2008 / Published online: 29 February 2008
© Springer Science+Business Media B.V. 2008

Abstract Variations of Earth's rotation rate (length-of-day, LOD) occur over a wide range of time scales from a few hours to the geological age. Studies showed that the 50-day fluctuation exists in LOD change. In the present paper, the authors use wavelet technique to study the 50-day oscillation in LOD series. Temporal variations of the oscillation are presented in this work. After analyzing the axial component of atmospheric angular momentum (AAM) and oceanic angular momentum (OAM), the 50-day periodic signal is also found in atmospheric and oceanic motion with remarkable time-variation. Meanwhile, the 50-day oscillation of the axial AAM is in good consistence with that of LOD change. This suggests that the 50-day oscillation of LOD change is mainly excited by the axial AAM. Possible origin of the oscillation for Earth system is discussed in the end of this paper.

Keywords Earth rotation · Atmospheric angular momentum · Oceanic angular momentum · Solar activity

1 Introduction

The variability of Earth-rotation vector is caused by gravitational torque exerted by the Sun, Moon and some other planets, mass redistribution in different parts of whole Earth system, and some other excitation mechanisms. The principle of conservation of angular momentum requires different variations taking place in different layers of the system. Earth's variable rotation with its complex movement state and excitation mechanism indicates the complexity of overall geodynamical process, and reflects the interaction courses among solid Earth, atmosphere and oceans, etc. In recent decades, modern space

L. Ma (✉) · Y. Han
National Astronomical Observatories, Chinese Academy of Sciences, Beijing 100012, China
e-mail: mlh@bao.ac.cn

D. Liao
Shanghai Astronomical Observatory, Chinese Academy of Sciences, Shanghai 200030, China

geodetic techniques (such as VLBI, SLR, LLR, GPS, etc.) have been routinely used to monitor the Earth's variable rotation and provided measurements with unprecedented precision and resolution, this allows for precise checking and studying of the dynamics of the Earth rotation. Analysis results from advanced data processing methods enable people to understand deeply variable characteristics of the Earth rotation (for a review, see, e.g., Lambeck 1980; Wahr 1988; Dickey et al. 1992; Dickey 1995).

Some studies have pointed out fluctuations in length-of-day (LOD), or Earth's rotation rate, with a period range from 40- to 60-day (intitled 50-day oscillation) (Zheng 1978; Feissel and Gambis 1980; Langley et al. 1981; Eubanks et al. 1985). The 40- to 60-day oscillation was first observed in tropical meteorological parameters by Madden and Julian (1971), and was characterized by Madden and Julian (1972) as being primarily variations in the zonal wind and mass fields that exhibited a definite phase propagation eastward and poleward in the tropical Indian Ocean and Pacific Ocean regions. After analyzing First GARP Global Experiment (FGGE) series from December of 1978 to November of 1979, Krishnamurti and Gadgil (1985) pointed out that the oscillation was a phenomenon existing in global atmospheric circulation. Meteorologists call the oscillation as Madden–Julian Oscillation. It's well known that the atmosphere is the principal excitation source of LOD change for periods from a few days up to a few years (Wilson 1995; Zhou and Zheng 2001; Gross et al. 2004; Ma et al. 2006a, b; 2007). The relations between LOD change and atmospheric motion on 40- to 60-day time scales have received considerable attention of astronomers and geophysicists. Hide et al. (1980) pointed out the axial component of atmospheric angular momentum (AAM) related to Earth rotation. Anderson and Rosen (1983) demonstrated that the 40- to 60-day variation in AAM was related to the tropical 50-day fluctuation. Barnes et al. (1983) considered AAM functions and gave transfer relation between AAM fluctuations and Earth's variable rotation. Madden (1987) gave a further link between the LOD and the 40- to 60-day atmospheric oscillation. Considering the combined effect of winds and surface pressure, Gross et al. (2004) thought that about 87% variance of intra-seasonal LOD variations can be explained by atmospheric excitation.

Using a band-pass filter, Anderson et al. (1984) study showed large temporal variations existing in the frequency and amplitude of the tropical 50-day oscillation. Li and Wilson (1987) treated 50-day oscillation as a damped oscillator by the random excitation, and concluded that the resonance periods changed with time. In order to understand deeply characteristics of Earth's variable rotation, here we use wavelet method to analyze the 40- to 60-day oscillation in LOD change, and discuss its possible excitation sources.

2 Data Sets

2.1 Length-of-day

The daily version of the SPACE2005 observed LOD series (Gross 2001) is used in this work. This series is derived from a combination of independent Earth orientation measurements taken by the space geodetic techniques of VLBI, SLR, LLR, and GPS, the Kalman filter used to combine the measurements also estimates its time rate-of-change and hence the LOD change (Gross et al. 1998). The SPACE2005 LOD series covers the period from September 28, 1976 to January 7, 2006. All Yoder solid Earth tides (including those longer than monthly) and long period oceanic tidal corrections to the Yoder model have been removed from this series. The LOD series with tidal effects removed is usually called as LODR.

In order to weaken the influence of end-effects during wavelet transform, EOPC04 series released from the International Earth Rotation and Reference System Service (IERS) is used to enlarge the LODR series after considering the systematic difference between EOPC04 and SPACE2005. After analyzing, the results are truncated to the original length of LODR time series.

2.2 Atmospheric Angular Momentum

Global atmospheric processes can be described by the effective atmospheric angular momentum (EAAM) functions. The axial component x_3 of EAAM functions, associated with LOD change, is composed of wind terms integrated over all latitude and longitude grids, and mass terms integrated over all latitude, longitude grids and pressure layers from surface to top of the model. Corresponding formula is as follows (Barnes 1983; Eubanks 1993).

$$\begin{aligned} \chi_3 = \chi_3^p + \chi_3^w = & \frac{0.753R^4}{C_m g} \int_0^{2\pi} \int_{-\pi/2}^{\pi/2} P_s \cos^3 \phi d\phi d\lambda \\ & + \frac{0.998R^3}{C_m \Omega g} \int_0^{2\pi} \int_{-\pi/2}^{\pi/2} \int_{P_s}^{P_{\text{top}}} u \cos^2 \phi dp d\phi d\lambda \end{aligned} \quad (1)$$

where, C_m is the axial moments of inertia of the mantle; R , Ω and g are the mean radius, mean rotation rate and gravity acceleration of the Earth; P_s and P_{top} are the surface pressure and the pressure at the top of model, u is the eastward wind velocities, respectively, λ and ϕ , longitude and latitude of each grid, and the coefficients 0.753 and 0.998 for x_3 take into consideration of the load deformation, rotational deformation and pole tide effects for the solid mantle, respectively.

For the axial AAM series, we use National Centers for Environmental Prediction/National Center for Atmospheric Research (NCEP/NCAR) reanalysis series during January 1, 1948–May 21, 2006 at 6 h interval. Wind terms integrated from surface to 10 hPa and mass terms with inverted barometer correction are used to form the axial component of AAM functions. The data set is first re-sampled at daily interval as that of the LOD variations.

2.3 Oceanic Angular Momentum

The oceanic angular momentum (OAM) series used in this work is the results of a simulation of the general circulation of the oceans done at JPL (Stammer et al. 2002). The ocean model used in this simulation is based on the MIT ocean general circulation model and has realistic boundaries and bottom topography (Marshall et al. 1997a, b). With 46 vertical levels ranging in thickness from 10 m at the surface to 400 m at depth using height as the vertical coordinate, the model spans the globe between 78 °S and 80 °N latitude with a latitudinal grid-spacing ranging from 1/3 degree at the equator to 1 degree at high latitudes and a longitudinal grid-spacing of 1 degree. The model is subsequently forced with 1949–2002 surface fluxes (twice daily wind stress, daily surface heat flux and evaporation-precipitation fields) from the NCEP/NCAR reanalysis project. Data set covers the period of time from January 1949 to December 2002 at 10 day intervals. Similar to AAM, OAM has three components composed of mass term (bottom pressure) and motion term (current), and the axial component of OAM is related to LOD variation.

2.4 Solar Activity Series

In order to study possible origin of the 50-day oscillation, we analyze active cavity radiometer irradiance monitor (ACRIM) composite total solar irradiance (TSI) time series for the period during November 16, 1978–October 1, 2003 by R. Willson. The ACRIM series is constructed from combinations of satellite TSI data sets. The Spline method is used to interpolate missing data.

Solar coronal index (SCI) of solar activity is measured by the total energy emitted by the Sun's outermost atmospheric layer (the corona) at a wavelength of 530.3 nm. It gives the radiant energy emitted by the entire visible corona within the Fe XIV spectral line—the emission from excited, ionized iron atoms. The SCI series is used to investigate solar activity for the years 1939–2004 with daily interval (Rybansky et al. 1994a, b).

As another important factor indicating solar activity, sunspot relative numbers (SSN) at daily interval during January 1, 1818–May 31, 2006 are downloaded from solar influences data analysis center (SIDC), and are studied.

3 Analysis

3.1 Wavelet Transform

By decomposing time series into time-frequency space, wavelet transform technique can lay out time variable information of signals in both time-domain and frequency-domain. The method is adapted to non-stationary time series, and has been used for numerous studies in geophysical, astronomical and other research fields. Details on wavelet method are described by some authors (Daubechies 1992; Chao and Natio 1995; Kumar and Foufoula-Georgiou 1997; Torrence and Compo 1998). In this study, we select Morlet wavelet as the mother wavelet.

3.2 Data Analysis and Comparison

Wavelet analyzing results of LODR series are shown in Fig. 1. The LODR series is given in the top of the figure. The following subfigure displays localized wavelet power spectra of LODR series. Considering that variable characteristics of LOD change on 40- to 60-day time scales are studied in this work, wavelet scales are adopted from 32- to 64-day with spectra lined out with contour in the figure, where, the alternation between the red and blue lines denotes intensities of the LOD wavelet power spectra on 32- to 64-day time scales, time sects with strong energy have higher color saturation. Undoubtedly, the 50-day fluctuation exists in LODR series, meanwhile, the oscillation is a quasi-periodic signal with obvious time-variable characteristics. That is to say, their periodic length and amplitude both change with time. From the figure, wavelet power of the 50-day oscillation in about 1981, 1988, 1990, 1997 and 2002, is relative stronger than other time sects. Similar to LOD change, wavelet transform of the axial AAM is calculated and the result is drawn in the third subfigure of Fig. 1.

Under conservation of angular momentum for the whole Earth system, the effects of the axial OAM can also raise LOD change (Johnson et al. 1999; Ponte et al. 2000, 2002). More LOD variations are excited after considering atmospheric and oceanic influence on LOD. Here, we calculate wavelet transform of 40- to 60-day fluctuation for the axial OAM change, and plot the results in the bottom of Fig. 1.

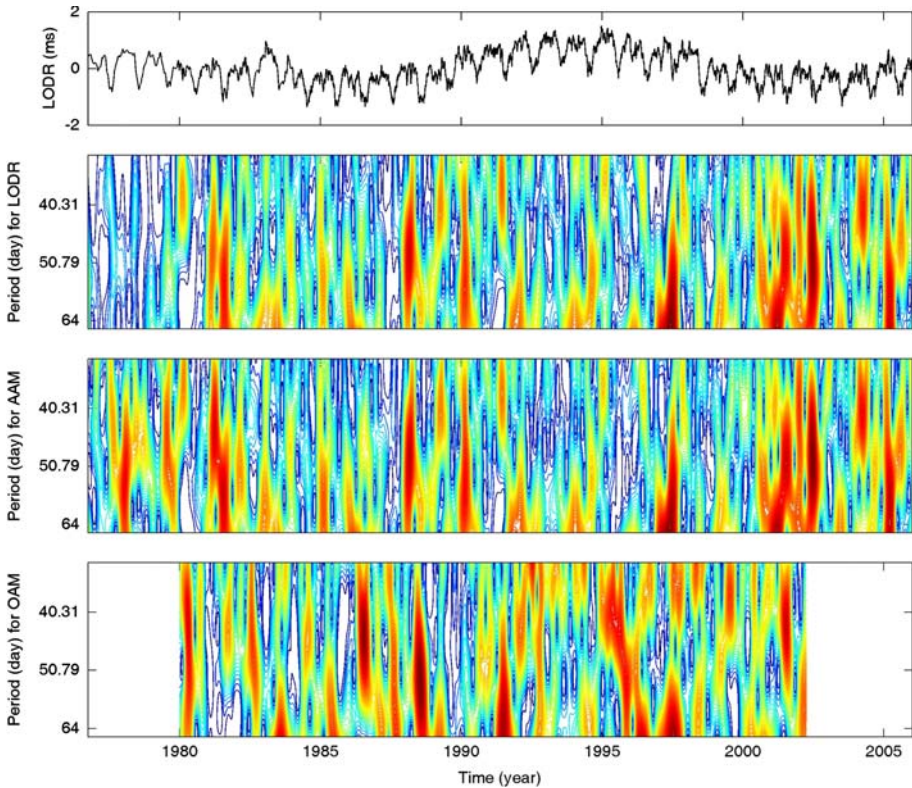


Fig. 1 Wavelet power spectrum of LODR, AAM and OAM series with 32- to 64-day wavelet scales. The four subfigures from top to bottom are corresponding to LODR series, LODR wavelet spectrum, AAM wavelet spectrum and OAM wavelet spectrum, respectively. In wavelet spectrum, the left axis is the Fourier period (in day) corresponding to the wavelet scale and the bottom axis is time (in year)

From the first two subfigures of Fig. 1, wavelet spectrum of the axial of AAM series is much similar to that of the axial of LOD change on 32- to 64-day time scales. Meanwhile, the oscillation has similar time-variable characteristics. In order to confirm relationship between the axial AAM and LOD change on 40- to 60-day time scales, we calculate their scale-averaged wavelet power. The corresponding formula is the following (Torrence and Compo 1998).

$$\bar{W}_n^2 = \frac{\delta j \delta t}{C_\delta} \sum_{j=j_1}^{j_2} \frac{|W_n(s_j)|^2}{s_j} \tag{2}$$

where, $|W_n(s)|^2$ is scale-averaged wavelet power over scales s_1 to s_2 , for Morlet wavelet, $C_\delta = 0.776$. Scale-averaged wavelet power for period of about 50 days of the axial AAM and LODR is calculated and corresponding results are plotted in Fig. 2a.

Scale-averaged variances of the axial AAM are in good consistence with ones of LODR. There are many peaks in scale-averaged variances of LODR and the axial AAM in Fig. 2a. Especially, their scale-averaged variances reach maximum during 1988–1989 and 1997–1998, corresponding to the very strong La Nina and El Nino events happened during these periods, respectively. However, similar connection is not clear among other peaks. Possible

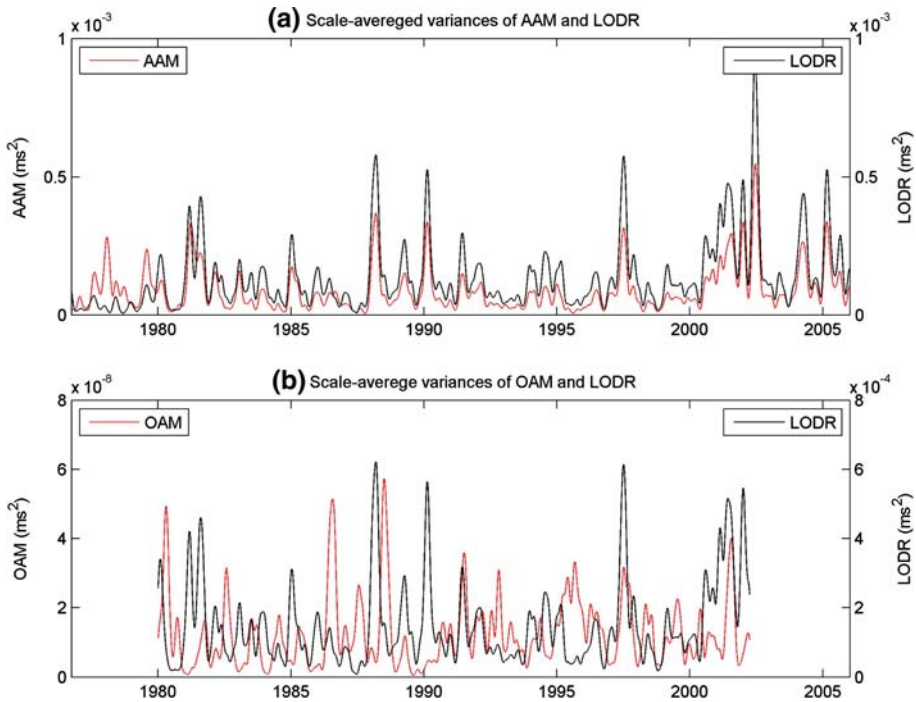


Fig. 2 Scale-averaged variances of the wavelet power for the time scales from 40- to 60-day. It gives mean energy of the wavelet spectra at each time epoch. Upper and lower panels are from AAM & LODR, OAM & LODR, respectively

reasons of difference of frequency spectrum on 40- to 60-day time scales between LOD and AAM before 1980 maybe result from being lack of high precise observatories from sufficient geodetic techniques.

From the bottom subfigure of Fig. 1, the 50-day fluctuation exists in the axial OAM, too. Meanwhile, the fluctuation has obvious time-variable characteristics. Power spectra of OAM on 40- to 60-day oscillation reach maximum in about 1982, 1988, 1997 and 2002. Furthermore, we calculate scale-averaged variances of the axial OAM on 40- to 60-day fluctuation and plot results with red solid line in Fig. 2b, the scale-averaged variances of the 50-day oscillation for LODR series during the period of time are the same as that of OAM and drawn with black solid line in Fig. 2b. Variances of OAM also reach maximum during some periods of time, however, peaks time of the axial OAM and LOD change have obvious difference. From the Fig. 2, the 50-day oscillation of LODR is quite different from that of the axial of OAM, and weak connection is obvious in their variations.

From above analysis, it strongly suggests that almost all of the changes of LOD on 40- to 60-day time scales are excited by the variations in the axial AAM.

4 Conclusion and Discussion

Results from wavelet analysis show time-variable characteristics in 40- to 60-day fluctuation of LOD change. Frequency and amplitude of the 50-day oscillation change with time. Analyzing the 50-day oscillation of the axial AAM, we find that good consistence exists in

LOD change and the axial AAM. The oscillation of the axial AAM can explain most parts of variances of the LOD during 1976–2006. Excitation contribution from the axial OAM is less. The unexplained part of the 50-day oscillation variance in LOD is mainly from some other excitation sources, such as upper atmospheric winds, hydrological processes etc.

Some studies showed the 50-day fluctuation exists in some geophysical phenomena including solar activity. Comparison from classical methods displays that oscillations of solar activity are similar to those of the atmospheric circulation. Some authors argued solar activity is the origin of the 50-day oscillation among geophysical events (Djurovic and Paquet 1988; Djurovic et al. 1994; Gu and Zheng 1992; Gu and Paquet 1995; Li et al. 1996). Here, we calculate wavelet spectrum of several time series of solar activity including solar irradiance, solar coronal index, and sunspot relative numbers. Corresponding results are shown in Fig. 3.

From Fig. 3, these time series of solar activity have similar variable characteristics. Compared with 27-day fluctuation, the 50-day period is weak, even weaker than ~ 85 -day fluctuation in some solar cycles. Furthermore, combining wavelet spectrum of the 50-day period for the axial AAM change, we find complicated variations in the oscillation of solar activity. Specially, the high-frequency oscillations get stronger (weaker) when solar activity becomes strong (weak). However, we can't find this point form the 50-day oscillation of the axial AAM change, and there is a little comparability between the axial AAM and solar activity. Obvious connection between atmosphere and solar activity on 40- to 60-day oscillation is not found. The results of wavelet analysis show that solar

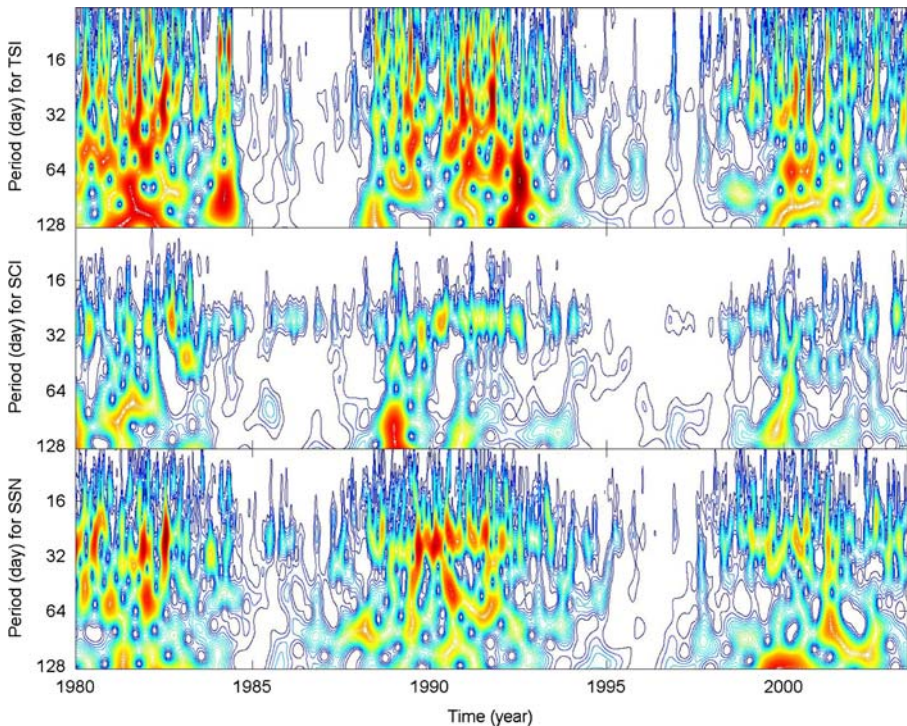


Fig. 3 Wavelet power spectra of TSI (top), SCI (middle) and SSN (bottom) series on scales of 8- to 128-day during 1980–2004

activity doesn't directly influence atmospheric motion on 40- to 60-day time scales. If solar activity impacts atmospheric process to some extent, the corresponding physical mechanism is very complicated, and attention should be paid to it when studying the 50-day oscillation in Earth rotation.

Acknowledgements The authors are grateful to IERS and NCEP/NCAR for providing EOPC04 and AAM series, respectively, to R. A. M. Van der Linden and the SIDC team for providing catalogue of the sunspot index. The manuscript was improved by suggestions of Angelo Poma. Wavelet software is provided by C. Torrence and G. Compo, and is available at URL: <http://www.paos.colorado.edu/research/wavelets/>. The work is supported by the National Natural Science Foundation of China under Grant 10373017.

References

- J.R. Anderson, R.D. Rosen, *J. Atmos. Sci.* **40**(6), 1584 (1983)
 J.R. Anderson, D.E. Stevens, P.R. Julian, *Mon. Weather Rev.* **112**(12), 2431 (1984)
 R.T.H. Barnes, R. Hide, A.A. White, C.A. Wilson, *Proc. R. Soc. Lond, Ser. A.* **387**, 31 (1983)
 B.F. Chao, I. Naito, *EOS, Trans. Am. Geophys. Union* **76**, 161 (1995)
 I. Daubechies, *Ten Lectures on Wavelets* (SIAM, Philadelphia, 1992)
 J.O. Dickey, *Global Earth Physics: A Handbook of Physical Constants*, ed. by T.J. Ahrens (AGU, Washington DC, 1995)
 J.O. Dickey, S.L. Marcus, J.A. Steppe, R. Hide, *Science* **255**, 321 (1992)
 D. Djurovic, P. Paquet, A. Billiau, *Astron. Astrophys.* **204**(1–2), 306 (1988)
 D. Djurovic, P. Paquet, A. Billiau, *Astron. Astrophys.* **288**(1), 335 (1994)
 T.M. Eubanks, *Geodyn Ser. 24*, ed. by D.E. Smith, D.L. Turcotte (AGU, Washington DC, 1993), p.1
 T.M. Eubanks, J.A. Steppe, J.O. Dickey, P.S. Callahan, *J. Geophys. Res.* **90**, 5385 (1985)
 M. Feissel, D. Gambis, *C. R. Acad. Sci. Paris.* **291**, 271 (1980)
 R.S. Gross, *JPL Publ.* **1–2**, 25 (2001)
 R.S. Gross, T.M. Eubanks, J.A. Steppe, A.P. Freedman, J.O. Dickey, T.F. Runge, *J. Geod.* **72**, 215 (1998)
 R.S. Gross, I. Fukumori, D. Menemenlis, P. Gegout, *J. Geophys. Res.* **109**, B01406 (2004)
 H. Gu, D.W. Zheng, *Ann. Shanghai observatory* **12**, 13 (1992)
 Z.N. Gu, P. Paquet, *Acta Astronomica Sinica* **36**(1), 65 (1995)
 R. Hide, N.T. Birch, L.V. Morrison, D.J. Shea, A.A. White, *Nature* **286**, 114 (1980)
 T.J. Johnson, C.R. Wilson, B.F. Chao, *J. Geophys. Res.* **104**, 25183 (1999)
 T.N. Krishnamurti, S. Gadgil, *Tellus* **37A**, 336 (1985)
 P. Kumar, E. Foufoula-Georgiou, *Rev. Geophys.* **35**(4), 385 (1997)
 K. Lambeck, *The Earth's Variable Rotation* (Cambridge Univ. Press, Cambridge, 1980)
 R.B. Langley, R.W. King, I.I. Shapiro, et al., *Nature* **294**, 730 (1981)
 Z.A. Li, C.R. Wilson, *Acta Astronomica Sinica* **28**, 29 (1987)
 Z.A. Li, Q. Lin, Y.B. Han, J. Zhao, *Acta Astronomica Sinica* **37**(4), 443 (1996)
 L.H. Ma, *Observatory* **127**, 364 (2007)
 L.H. Ma, Y.B. Han, *Chin. J. Astron. Astrophys.* **6**, 120 (2006a)
 L.H. Ma, D.C. Liao, Y.B. Han, *Chin. J. Astron. Astrophys.* **6**, 759 (2006b)
 R.A. Madden, *J. Geophys. Res.* **92**, 8391 (1987)
 R.A. Madden, P.R. Julian, *J. Atmos. Sci.* **28**, 702 (1971)
 R.A. Madden, P.R. Julian, *J. Atmos. Sci.* **29**, 1109 (1972)
 J. Marshall, C. Hill, L. Perelman, A. Adcroft, *J. Geophys. Res.* **102**(C3), 5733 (1997a)
 J. Marshall, A. Adcroft, C. Hill, L. Perelman, C. Heisey, *J. Geophys. Res.* **102**(C3), 5753 (1997b)
 R.M. Ponte, D. Stammer, *J. Geophys. Res.* **105**, 17161 (2000)
 R.M. Ponte, J. Rajamony, J.M. Gregory, *Clim. Dyn.* **19**, 181 (2002)
 M. Rybansky, V. Rusin, M. Minarovjeh, P. Gaspar, *Sol. Phys.* **152**, 153 (1994a)
 M. Rybansky, V. Rusin, P. Gaspar, C. Richard, *Sol. Phys.* **152**, 487 (1994b)
 D. Stammer, C. Wunsch, I. Fukumori, J. Marshall, *EOS, Trans. AGU.* **83**(27), 289 (2002)
 C. Torrence, G. Compo, *Bull. Am. Meteor. Soc.* **79**, 61 (1988)
 J.M. Wahr, *Annu. Rev. Earth Planet. Sci.* **16**, 231 (1988)
 C.R. Wilson, *Rev. Geophys.(suppl.)* **33**, 225 (1995)
 D.W. Zheng, *Acta Astronomica Sinica* **19**, 103 (1978)
 Y.H. Zhou, D.W. Zheng, N.H. Yu, X.H. Liao, *Chin. Sci. Bull.* **46**(11), 881 (2001)